This document is the accepted manuscript version of the following article:
Witte, K., Mantouvalou, I., Sánchez-De-Armas, R., Lokstein, H., Lebendig-Kuhla, J., Jonas, A., … Stiel, H. (2018). On the electronic structure of Cu chlorophyllin and its breakdown products: a carbon K-edge X-ray absorption spectroscopy study. Journal of Physical Chemistry B, 122(6), 1846-1851. https://doi.org/10.1021/acs.jpcb.7b12108

On the Electronic Structure of Cu-Chlorophyllin and its Breakdown Products – a Carbon K-edge X-ray Absorption Spectroscopy Study

Katharina Witte[*,†,&], *Ioanna Mantouvalou*[†,&], *Rocío Sánchez-de-Armas*[‡], *Heiko Lokstein*[#], *Janina Lebendig-Kuhla*[†,‖,&], *Adrian Jonas*[†,&], *Friedrich Roth*[▲], *Birgit Kanngießer*[†,&], and *Holger Stiel*[‖,&]

AUTHOR ADDRESS

[†] Technische Universität Berlin, Institut für Optik und Atomare Physik, 10623 Berlin, Germany

[&] Berlin Laboratory for innovative X-ray technologies (BLiX), 10623 Berlin, Germany

[‡] Uppsala University, Department of Physics and Astronomy, Materials Theory Division, P.O. BOX 516, S75120 Uppsala, Sweden

[#] Charles University, Faculty of Mathematics and Physics, Department of Chemical Physics and Optics, Ke Karlovu 3, 121 16 Prague, Czech Republic

[▲]Technische Universität Bergakademie Freiberg, Institut für Experimentelle Physik, Leipziger Strasse 23, 09599 Freiberg, Germany

[‖] Max-Born-Institut für Nichtlineare Optik und Kurzzeitspektroskopie Berlin, 12489 Berlin, Germany

AUTHOR INFORMATION

Corresponding Author

*E-mail: katharina.witte@psi.ch

ABSTRACT.

Using Near-Edge X-ray Absorption Fine Structure Spectroscopy (NEXAFS) the carbon backbone of sodium copper chlorophyllin (SCC), a widely used chlorophyll derivative, and its breakdown products are analyzed to elucidate their electronic structure and physicochemical properties. Using various sample preparation methods and complementary spectroscopic methods (including UV/VIS, X-ray Photoelectron Spectroscopy), a comprehensive insight into the SCC breakdown process is presented. The experimental results are supported by Density Functional Theory (DFT) calculations allowing a detailed assignment of characteristic NEXAFS-features to specific C-bonds. SCC can be seen as a model system for the large group of porphyrins, thus this work provides a novel and detailed description of the electronic structure of the carbon backbone of those molecules and their breakdown products. The achieved results also promise prospective optical pump - X-ray probe investigations of dynamic processes in chlorophyll containing photosynthetic complexes to be analyzed more precisely.

KEYWORDS (Copper) chlorophyllin, breakdown products, electronic structure, UV/VIS spectroscopy, Carbon K-edge, NEXAFS, DFT

INTRODUCTION

The role of chlorophylls (Chl) in photosynthetic light-harvesting processes and energy conversion has been studied extensively in the past[1-3] in order to elucidate, understand or even mimic nature's mechanisms. Structure-function relationships in pigment-protein complexes containing Chl molecules are currently in the focus of research, since efficient light-energy conversion is one of the grand challenges of our time[4]. Under certain developmental and/or environmental conditions (higher) plants as well as algae and cyanobacteria degrade Chl molecules actively[5]. Chl breakdown in plants first requires uncoupling of the molecules from the Chl-binding protein. Subsequently, the Chl molecules are converted in a multi-step process to structurally different catabolites. A widely visible sign of this process is the appearance of the autumn and/or ripe fruit colors. Some later Chl catabolites belong to colorless, bilane-type tetrapyrroles[6]. However, colored catabolites were also found in the Chl breakdown process[5]. Appearance and structure of these catabolites have been extensively studied, mainly by UV-VIS and NMR spectroscopy[6-7].

Sodium copper chlorophyllin ($C_{34}H_{31}CuN_4Na_3O_6$, SCC) is a semi-synthetic, water soluble derivative of Chl that is widely used in the food industry[8-10] and as a light absorber in organic photovoltaics[11-13]. Due to its characteristic tetrapyrrole structure, SCC can be regarded as a model system for the large group of porphyrins, of which Chl is one of most prominent and important, but by far not the only member. SCC can undergo (photo) chemical reactions in a manner very similar to that of Chl. A prominent example is a pink-colored breakdown intermediate[14].

Optical spectroscopy has been performed extensively on SCC[11-12], however, X-ray spectroscopic investigations, which render conclusions about the inner-shell electronic structure feasible are all

but missing[15]. With near edge X-ray absorption fine structure (NEXAFS) spectroscopy the electronic structure as well as the oxidation state can be probed. The use of soft X-ray radiation allows the investigation of the K absorption edges of carbon (C), oxygen (O) and nitrogen (N), as well as the L-edges of the central metal atom, thus providing a more comprehensive analysis of the entire SCC molecule. In this work a detailed description of the electronic structure of the C-backbone of SCC and its breakdown products is presented, based on experimental C K-edge NEXAFS data and Density Functional Theory (DFT) calculations.

EXPERIMENTAL AND COMPUTATIONAL METHODS

Sample preparation. Initially, SCC (commercial grade powder from Sigma Aldrich, no further purification) has been analyzed in a dried droplet (made from a solution in deionized H_2O, c = $2x10^{-3}$ mol/l) that can be seen as representative of the pristine molecular structure. Since the NEXAFS spectrum of the SCC droplet suffers from a low signal-to-noise ratio due to sample inhomogeneity (**Figure S1**) and to avoid contaminations as well, an SCC thin film has been produced using an effusion cell (EC, Createc Fischer & Co. GmbH). The latter is a common technique for producing thin layers of, e.g., phthalocyanine molecules[16]. The EC is integrated in a vacuum chamber, where pressures down to 10^{-7} mbar can be achieved. During the evaporation process the chamber pressure can increase up to $8x10^{-6}$ mbar. In contrast to phthalocyanines, the exact vaporization temperature of SCC is unknown. Thus, an optimization of the process using different heating rate sequences was conducted. As a result a total evaporation time of 3 h at a maximum temperature of about 300 °C were selected, yielding an optimum layer thickness for transmission NEXAFS spectroscopy of about (250 ± 50) nm.

Experimental Methods. Previously, the SCC samples were investigated by UV/VIS spectroscopy using a PerkinElmer Lambda900 spectrometer with a step size of 1 nm in the range between 300 and 800 nm. The molecular integrity and absorption behavior of the samples is verified by the characteristic absorption behavior of porphyrins[17].

To study the electronic structure of SCC and its breakdown products in more detail, NEXAFS investigations have been performed at the PolLux[18-21] beamline (X07DA) of the Synchrotron radiation facility Swiss Light Source (SLS) at the Paul Scherrer Institute (PSI), Villigen Switzerland, providing a high energy resolution in the required energy range ($E/\Delta E > 3000$ for E = 260 – 430 eV, see *Supporting Information*). Since the NEXAFS investigations were performed in transmission mode, thin Si_3N_4 membranes (d = 150 nm, Norcada Inc.) were used as substrates. The NEXAFS measurements were performed in the "line-scan" mode in a region of interest at the sample with a length between 4-6 µm (number of steps: 50, resulting in a spatial resolution between 0.08 µm and 0.12 µm). On each position, an energy scan consisting of 362 energy points with varying energy step sizes has been recorded (see **Table S1**). With a dwell time of 5 ms at each energy point, an overall acquisition time of 10 minutes per scan is needed.

Computational Methods. Density Functional Theory (DFT) calculations based on the gradient-corrected DFT program StoBe[22], with the exchange functional by Becke[23] and the correlation functional by Perdew[24], were used for the interpretation of the NEXAFS spectra. With a previously optimized SCC geometry the C K-edge NEXAFS spectrum was generated with StoBe for each C atom. The spectral intensities were generated from the computed transition dipole probabilities convoluted with Gaussian curves with increasing broadening from 0.5 – 5 eV. The total calculated NEXAFS spectrum for each compound was obtained by summing up all the single-atom 1s - 2p transitions.

Normalization of all NEXAFS spectra was done by using the program ATHENA Version 0.9.25[25]. Further details on the sample preparation, experimental methods and calculations are given in the *Supporting Information*.

RESULTS

After the evaporation process the resulting SCC thin film has turned color from dark green to red indicating a molecular alteration that can be confirmed by UV/VIS absorption spectroscopy (see **Figure 1, Table 1 and Figure S1**).

This rigorous color change can be explained by formation of breakdown products during heating. Catabolites and breakdown products occur in a large variety of molecular structures, e.g., as linear tetrapyrroles (*phyllobilins*[26]) with or without a central metal atom. Two important representatives are the yellow Chl-catabolites (YCC) and pink Chl-catabolites (PiCC)[27], which may among others be responsible for the colorful appearance of autumn leaves. Following the work of Kräutler *et al.*[28] we interpret the UV/VIS spectrum of the SCC thin film as a composite of multiple breakdown products.

Among a hypsochromic shift of the SCC thin film absorption spectrum, which argues against an aggregation of the SCC molecules[29] during the evaporation process, a further absorption band (UV-band) occurs around 320 nm and can be assigned to the absorption of the α-formyl pyrrole of *type-I phyllobilins*[28]. Although the Soret band around 400 nm can be explained by Gouterman`s four-orbital model for the optical absorption of porphyrins[17], characteristic Q-bands appear with a strong displacement and a pronounced double feature that cannot be explained by the splitting into the different Q-bands. These absorption bands occur below 550 nm for metal-

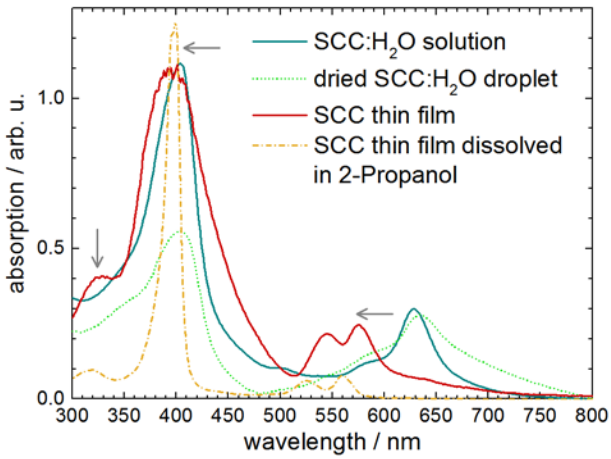

Figure 1. UV/VIS absorption spectra of SCC dissolved in water (turquoise), a dried SCC-water droplet (light green, dotted line), an evaporated SCC thin film (red) and an SCC thin film dissolved in 2-Propanol (orange, dash-dotted line). The spectral shifts and new arising absorption bands are indicated by arrows.

Table 1. UV/VIS absorption bands of various SCC samples

absorption band / sample	UV-band [i)]	Soret-band [i)]	Q-bands [i)]
SCC: H_2O	-	404 nm	628 nm
dried SCC solution	-	404 nm	634 nm
SCC thin film	325 nm	396 nm [ii)]	545 nm / 576 nm
dissolved SCC thin film	319 nm	399 nm	525 nm / 560 nm

i) The wavelengths of the absorption bands are given within an uncertainty of ±1 nm and ii) uncertainty of ±2 nm respectively .

free and above 550 nm for metal-containing PiCC molecules, respectively, in accordance with the results of Kräutler *et al*[28].

A further evidence for the existence of SCC breakdown products is the non-solubility of the SCC thin film in water. Additional XPS investigations (see **Figure S2**) pointed out that during the

evaporation process the weak ionic bonding between the Na^+ cations and the O^- anions breaks, which is responsible for the solubility in water.

To study the electronic structure of SCC and its breakdown products in more detail, NEXAFS investigations have been performed at the PolLux[18-21] beamline (X07DA) of the Synchrotron radiation facility Swiss Light Source (SLS) at the Paul Scherrer Institute (PSI), Villigen Switzerland, providing a high energy resolution in the required energy range ($E/\Delta E > 3000$ for E = 260 – 430 eV). Since the NEXAFS investigations were performed in transmission, thin Si_3N_4 membranes (d = 150 nm, Norcada Inc.) were used as substrates.

The C K-edge NEXAFS spectrum of a SCC droplet (green solid line) as shown in **Figure 2A** is characterized by small pre-edge features (peaks A & B) followed by two pronounced π* transitions D and E above 288 eV and a broad structure at higher energies around 300 eV. The detailed energetic positions are listed in **Table 2**. With regard to already published results[30-31] feature E can be assigned to a π* transition of the carbonate C=O bonding. This assignment can be confirmed using the C K-edge NEXAFS spectrum of dissolved sodium bicarbonate in water ($NaHCO_3$, **Figure 2A** blue dotted curve). This spectrum has been measured to aid further interpretation, using a laser produced plasma source[32] with a high resolution NEXAFS laboratory setup[33]. The $NaHCO_3$ spectrum displays a π* transition from the carbonate C=O bonding at 290 eV that can be also identified in the SCC NEXAFS signal and provides evidence for a carbonate contamination of the sample. Additionally, at energies above 295 eV, both NEXAFS spectra acquired at the synchrotron and in the laboratory, display the same characteristic features. This observation leads to the conclusion that the C K-edge NEXAFS spectrum of the SCC droplet can be interpreted as a superposition of the SCC and the $NaHCO_3$ NEXAFS signals generated by dissolving SCC in water.

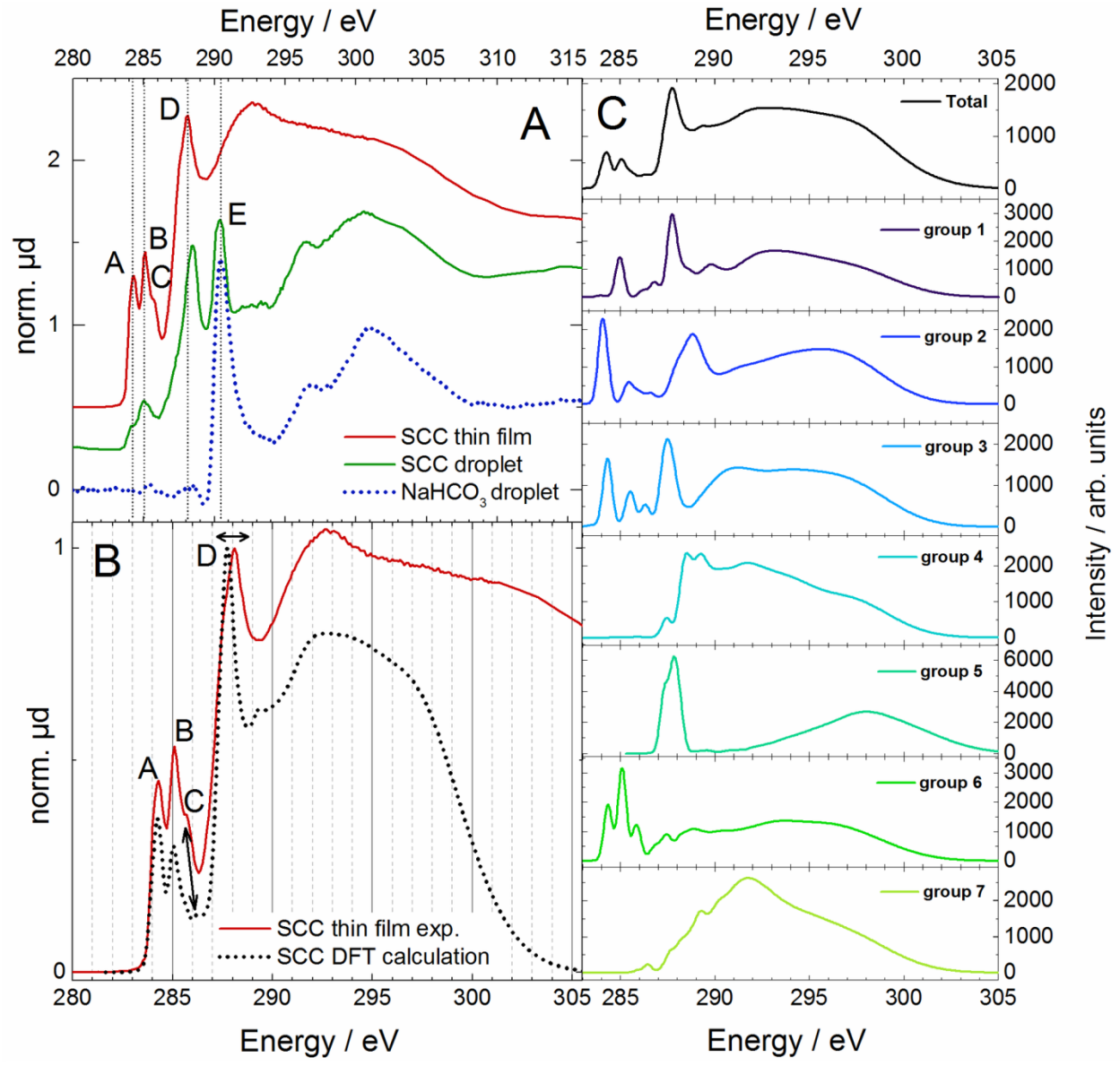

D

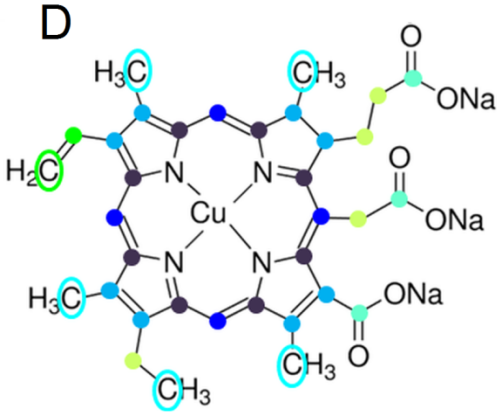

	chemical binding	peak contribution
group 1	C-N, C=N	B, C, D
group 2	-CH-, bound to two C`s within the porphyrin ring	A, B, C
group 3	C, bound to three C`s within the pyrrole ring	A, B, C, D
group 4	$-CH_3$	D
group 5	C-O, C=O	D
group 6	C=C, side chain	A, B, C
group 7	$-CH_2-$, side chains	> 290 eV

Figure 2. Normalized C K-edge NEXAFS spectra of an SCC droplet (green), an SCC thin film (red), an $NaHCO_3$ droplet (blue, dotted line) (A, B) and DFT-calculated spectra (B, C). The

NEXAFS spectra in A are displayed with an offset for clarification. The composition of the total DFT NEXAFS spectrum from the individual signals from specific C atoms of the SCC molecule is displayed in C. The molecular structure of SCC is shown in D, where the C-atoms are marked with regard to their chemical binding and peak contribution. The explanation of each group is given in the table.

Table 2. Resonance energies of experimental and DFT-calculated NEXAFS spectra.

Peak	SCC droplet [i)]	SCC thin film [i)]	DFT
A	284.1	284.2	284.2
B	285.0	285.0	285.0
C	-	285.4	286.3
D	288.6	288.2	287.8
E	290.4	-	-

i) The experimentally determined energies are given with an uncertainty of ±0.1 eV caused by the step size.

These results are an excellent example, how synchrotron- and laboratory-based investigations can complement each other.

In comparison, the SCC thin film NEXAFS signal features the same characteristic peaks with similar energetic positions as the previously discussed SCC droplet NEXAFS (**Table 2**). However, the intensities of the pre-edge structures (peaks A & B) are increased with regard to the π*-resonance (peak D) and the intensity ratio changes significantly. Additionally, a slight shoulder towards higher energies (peak C at 285.5 eV) can be resolved. A carbonate contamination is not detectable.

Surprisingly, the DFT calculations (**Figure 2B** & **C**) based on the pristine SCC molecular structure very well reproduce at least the pronounced peaks A, B for both, SCC droplet and thin film (**Figure 2C** & **D**). The two pre-edge features, peaks A and B, mainly originate from C=C and C-C bonds within the tetrapyrrole ring (*group 2* & *3*) of SCC, whereas peak B has an

additional contribution from C atoms bound to N atoms (*group 1*). The higher intensity of peak B in relation to peak A in the measured spectrum can be attributed to a larger proportion of C-N and C=N bonds, which in turn is another evidence for the presence of catabolites and degradation products, in which the bonding to the central metal ion is no longer present. The DFT calculations for the intact SCC molecular structure suggest that the intensity ratio should be exactly the opposite.

Feature C, which is clearly visible in the thin film NEXAFS spectrum, can be attributed to similar C bonds as peaks A and B but with much lower intensity.

Moreover, the experimental and theoretical results listed in **Table 2** show large deviations that make a clear assignment difficult. Towards higher energies, feature D can be assigned to C=O and C-O bonds. For this resonance a shift towards higher energies occurs in the order: DFT calculations, SCC thin film and SCC droplet. This shift can be explained by the increasing influence of additional oxygen, either by a change of the molecular structure (thin film) or a contamination (droplet). These “external contributions” are not taken into account in the DFT calculations, as well as the C 1s edge jump, which explains the trend of the calculated spectrum above 290 eV.

The previously shown UV/VIS spectra indicate that several breakdown products should be present in the SCC thin film. However, the fact that the DFT calculations, even though they are based on the pristine SCC molecular structure, reproduce the near edge region of the NEXAFS spectra with high precision, can be explained by the chemical bonds that are responsible for these characteristic NEXAFS structures. For linear tetrapyrroles or open-ring catabolites, extended conjugated π-electron systems are present.

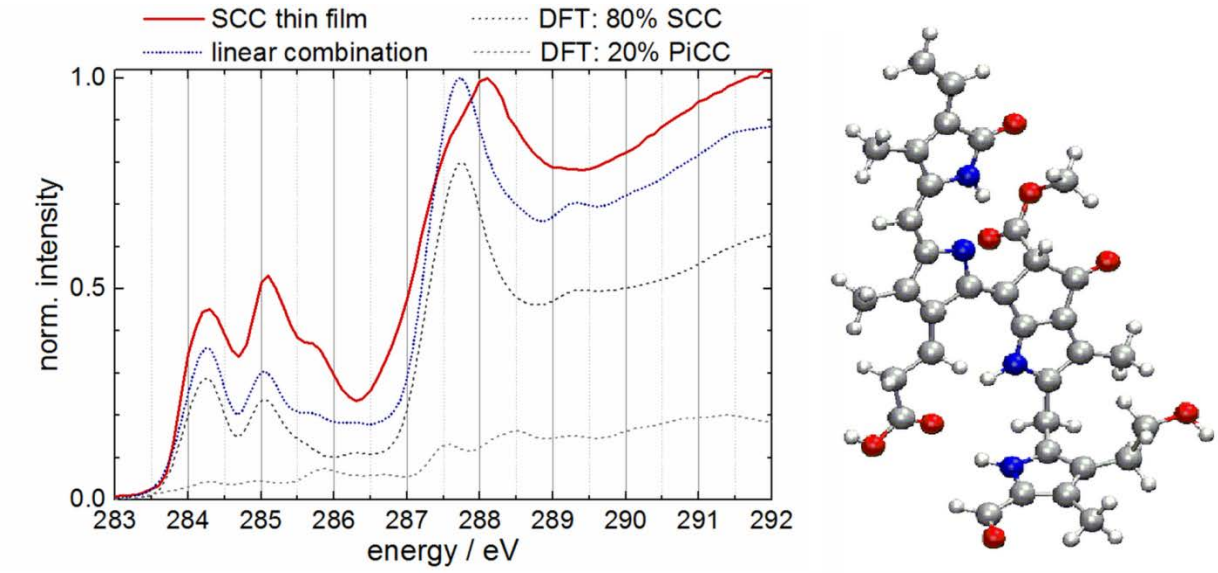

Figure 3. Left: SCC thin film NEXAFS spectrum (red solid line) in comparison to a linear combination (navy-blue dotted line) of DFT calculated spectra of SCC (80%, dark grey dotted line) and one of its catabolites, the pink chlorophyll catabolite (20% PiCC, grey dotted line). Right: molecular structure of the PiCC molecule (white: H, grey: C, blue: N, red: O).

The NEXAFS spectrum of the thin film is shown in comparison to the DFT calculated spectra of SCC (dark grey, dotted line) and PiCC (grey, dotted line) in **Figure 3**. The two calculated spectra of SCC and PiCC are additionally shown in **Figure S3** in the *Supporting Information*. While the single spectra of both components can explain parts of the experimental results, a linear combination (dark blue, dotted line) of the ratio 80 % SCC to 20 % PiCC leads to a better agreement between the calculations and the measured data especially in the pre-edge region. Thus, feature C at 285.5 eV can now be explained by the existence of PiCC in the thin film. However, these calculations also show that only one additional structure is not sufficient to reproduce the entire NEXAFS spectrum of the thin film.

CONCLUSION

Due to the large number of possible different breakdown products, additional analysis such as nuclear magnetic resonance (NMR)[34], which are beyond the scope of this work, will be necessary to identify further components and to perform additional DFT calculations. Furthermore, the partial nonconformity between the SCC droplet NEXAFS spectrum and the calculated DFT spectrum remains an open question and requires further considerations. Nevertheless, the X-ray spectroscopic analysis of commercial grade SCC in combination with the presented DFT calculations provides a novel and detailed description of the electronic structure of this widely used molecule and its breakdown products. The presented results are the first X-ray spectroscopic investigations of the carbon skeleton of the SCC molecule and its breakdown products supported by DFT calculations. Using a VIS pump/X-ray probe experimental arrangement additional NEXAFS resonances due to a vacancy in the HOMO of the molecule can be generated[35]. These resonances should be visible in the NEXAFS spectra as characteristic fingerprints of different catabolite structures. Such experiments, allowing a further differentiation between the catabolites are planned for the near future.

ASSOCIATED CONTENT

Supporting Information. The following files are available free of charge.

Sample preparation, sample images, details about the PolLux beamline and BLiX LPP source, details of DFT calculations, details about XPS measurements. DFT calculations PiCC & SCC (PDF)

AUTHOR INFORMATION

Corresponding Author

Dr. Katharina Witte

Current affiliation: Paul Scherrer Institute, 5232 Villigen, Switzerland

Notes

The authors declare no competing financial interests.

ACKNOWLEDGMENT

We would like to thank Katrin Hermann (Max-Born-Institute) for the support with the UV/VIS measurements and Dr. Benjamin Watts for giving us the opportunity to perform the NEXAFS measurements at the PolLux beamline at SLS. The PolLux end station was financed by the German Minister für Bildung und Forschung (BMBF) through contracts 05KS4WE1/6 and 05KS7WE1. The current position of KW at PSI has received funding from the European Union`s Horizon 2020 research & innovation programme under the Marie Skłodowska-Curie grant agreement No 701647 (PSI Fellowship). H.L. acknowledges support by the Czech Science Foundation. GAČR (#P501/12/G055). The current affiliation of RSA is University of Seville, Faculty of Pharmacy, Department of Physical Chemistry, 41004 Seville, Spain.

REFERENCES

(1) Reimers, J. R.; Biczysko, M.; Bruce, D.; Coker, D. F.; Frankcombe, T. J.; Hashimoto, H.; Hauer, J.; Jankowiak, R.; Kramer, T.; Linnanto, J. et al Challenges facing an understanding of the nature of low-energy excited states in photosynthesis. *Biochimica et Biophysica Acta (BBA) - Bioenergetics* **2016,** *1857* (9), 1627-1640.
(2) Qin, X.; Suga, M.; Kuang, T.; Shen, J.-R. Structural basis for energy transfer pathways in the plant PSI-LHCI supercomplex. *Science* **2015,** *348* (6238), 989-995.
(3) Muh, F.; Renger, T. Refined structure-based simulation of plant light-harvesting complex II: Linear optical spectra of trimers and aggregates. *Bba-Bioenergetics* **2012,** *1817* (8), 1446-1460.
(4) Blankenship, R. E.; Tiede, D. M.; Barber, J.; Brudvig, G. W.; Fleming, G.; Ghirardi, M.; Gunner, M. R.; Junge, W.; Kramer, D. M.; Melis, A. e. a. Comparing Photosynthetic and Photovoltaic Efficiencies and Recognizing the Potential for Improvement. *Science* **2011,** *332* (6031), 805-809.
(5) Christ, B.; Hörtensteiner, S. Mechanism and Significance of Chlorophyll Breakdown. *Journal of Plant Growth Regulation* **2014,** *33* (1), 4-20.
(6) Li, C.; Ulrich, M.; Liu, X.; Wurst, K.; Muller, T.; Krautler, B. Blue transition metal complexes of a natural bilin-type chlorophyll catabolite. *Chemical Science* **2014,** *5* (9), 3388-3395.
(7) Kräutler, B. Phyllobilins - the abundant bilin-type tetrapyrrolic catabolites of the green plant pigment chlorophyll. *Chemical Society Reviews* **2014,** *43* (17), 6227-6238.
(8) Kephart, J. C. Chlorophyll derivatives—Their chemistry, commercial preparation and uses. *Economic Botany* **1955,** *9* (1), 3.
(9) Hendry G. A. F.; Houghton, J. D. *Natural Food Colorants*. Dordrecht, 1996.
(10) Tumolo, T.; Lanfer-Marquez, U. M. Copper chlorophyllin: A food colorant with bioactive properties? *Food Research International* **2012,** *46* (2), 451-459.
(11) Aydin, M. E.; Farag, A. A. M.; Abdel-Rafea, M.; Ammar, A. H.; Yakuphanoglu, F. Device characterization of organic nanostructure based on sodium copper chlorophyllin (SCC). *Synthetic Metals* **2012,** *161* (23-24), 2700-2707.
(12) Farag, A. A. Optical absorption of sodium copper chlorophyllin thin films in UV-vis-NIR region. *Spectrochim Acta A Mol Biomol Spectrosc* **2006,** *65* (3-4), 667-72.
(13) Calogero, G.; Citro, I.; Crupi, C.; Di Marco, G. Absorption spectra and photovoltaic characterization of chlorophyllins as sensitizers for dye-sensitized solar cells. *Spectrochim Acta A Mol Biomol Spectrosc* **2014,** *132*, 477-84.
(14) Oster, G.; Bellin, J. S.; Broyde, S. B. Photochemical Properties of Chlorophyllin Alpha. *J. Am. Chem. Soc.* **1964,** *86* (7), 1313-1318.
(15) Nagatani, H., Tanida, H.; Watanbe, I.; Sagara, T. Extended X-ray Absorption Fine Structure of Copper(II) Complexes at the Air–Water Interface by a Polarized Total-Reflection X-ray Absorption Technique. *ANALYTICAL SCIENCES* **2009,** *25*, 475-480.
(16) Willey, T. M.; Bagge-Hansen, M.; Lee, J. R.; Call, R.; Landt, L.; van Buuren, T.; Colesniuc, C.; Monton, C.; Valmianski, I.; Schuller, I. K. Electronic structure differences between H(2)-, Fe-, Co-, and Cu-phthalocyanine highly oriented thin films observed using NEXAFS spectroscopy. *J Chem Phys* **2013,** *139* (3), 034701.

(17) Gouterman, M. Spectra of porphyrins. *Journal of Molecular Spectroscopy* **1961,** *6* (Supplement C), 138-163.
(18) Flechsig, U., Quitmann, C.; Raabe,J.; Böge, M.; Fink, R.; and Ade, H. The PolLux Microspectroscopy Beamline at the Swiss Light Source. *AIP Conference Proceedings* **2006,** *879*, 505-508.
(19) Raabe, J.; Tzvetkov, G.; Flechsig, U.; Boge, M.; Jaggi, A.; Sarafimov, B.; Vernooij, M. G.; Huthwelker, T.; Ade, H.; Kilcoyne, D.; Tyliszczak, T.; Fink, R. H.; Quitmann, C. PolLux: a new facility for soft x-ray spectromicroscopy at the Swiss Light Source. *Rev Sci Instrum* **2008,** *79* (11), 113704.
(20) Henein, S.; Frommherz, U.; Betemps, R.; Kalt, H.; Ellenberger, U.; Flechsig, U.; Raabe, J. Mechanical Design of a Spherical Grating Monochromator for the Microspectroscopy Beamline PolLux at the Swiss Light Source. *AIP Conference Proceedings* **2007,** *879* (1), 643-646.
(21) Frommherz, U.; Raabe, J.; Watts, B.; Stefani, R.; Ellenberger, U. Higher Order Suppressor (HOS) for the PolLux Microspectroscope Beamline at the Swiss Light Source SLS. *AIP Conference Proceedings* **2010,** *1234* (1), 429-432.
(22) Hermann, K.; Petterson, L. *StoBe-deMon, version 3.0*, 2007.
(23) Becke, A. D. Density-functional exchange-energy approximation with correct asymptotic behavior. *Physical Review A* **1988,** *38*, 3098-3100.
(24) Perdew, J. P. Erratum: Density-functional approximation for the correlation energy of the inhomogeneous electron gas. *Physical Review B* **1986,** *34*, 7406.
(25) Ravel, B., Newville, M. . ATHENA, ARTEMIS, HEPHAESTUS: Data Analysis for X-ray Absorption Spectroscopy using IFEFFIT. *Journal of Synchrotron Radiation* **2005,** *12*, 537 - 541.
(26) Li, C., Wurst, K., Jockusch, S., Gruber, K., Podewitz, M., Liedl, K. R., Kräutler, B. Chlorophyll-Derived Yellow Phyllobilins of Higher Plants as Medium-Responsive Chiral Photoswitches. *Angewandte Chemie (International ed. in English)* **2016,** *55*, 15760 - 15765.
(27) Li, C., Ulrich, M., Liu, X., Wurst, K., Müller, T., Kräutler, B. Blue transition metal complexes of a natural bilin-type chlorophyll catabolite. *Chemical Science* **2014,** *5*, 3388 - 3395.
(28) Kräutler, B. Phyllobilins--the abundant bilin-type tetrapyrrolic catabolites of the green plant pigment chlorophyll. *Chem Soc Rev* **2014,** *43* (17), 6227-38.
(29) Frackowiak, D. Z., B.; Helluy, A.; Niedbalska, M.; Goc, J.; Leblanc, R. M. Aggregation of chlorophylls a and b in polymer films and monolayers. *J. Photochem. Photobiol. A: Chem.* **1992,** *69*, 213-222.
(30) Urquhart, S. G., Ade, H. Trends in the Carbonyl Core (C 1S, O 1S) → pi* C=O Transition in the Near-Edge X-ray Absorption Fine Structure Spectra of Organic Molecules. *Journal of Physical Chemistry B* **2002,** *106*, 8531 - 8538.
(31) Espinal, L.; Green, M. L.; Fischer, D. A.; DeLongchamp, D. M.; Jaye, C.; Horn, J. C.; Sakwa-Novak, M. A.; Chaikittisilp, W.; Brunelli, N. A.; Jones, C. W. Interrogating the Carbon and Oxygen K-Edge NEXAFS of a CO2-Dosed Hyperbranched Aminosilica. *J Phys Chem Lett* **2015,** *6* (1), 148-52.
(32) Mantouvalou, I.; Witte, K.; Grötzsch, D.; Neitzel, M.; Günther, S.; Baumann, J.; Jung, R.; Stiel, H.; Kanngiesser, B.; Sandner, W. High average power, highly brilliant laser-produced plasma source for soft X-ray spectroscopy. *Rev Sci Instrum* **2015,** *86* (3), 035116.

(33) Mantouvalou, I.; Witte, K.; Martyanov, W.; Jonas, A.; Grötzsch, D.; Streeck, C.; Löchel, H.; Rudolph, I.; Erko, A.; Stiel, H.; Kanngießer, B. Single shot near edge x-ray absorption fine structure spectroscopy in the laboratory. *Applied Physics Letters* **2016,** *108* (20), 201106.
(34) Ulrich, M.; Moser, S.; Müller, T.; Kräutler, B. How the Colourless 'Nonfluorescent' Chlorophyll Catabolites Rust. *Chemistry – A European Journal* **2011,** *17* (8), 2330-2334.
(35) Wolf, T. J. A.; Myhre, R. H.; Cryan, J. P.; Coriani, S.; Squibb, R. J.; Battistoni, A.; Berrah, N.; Bostedt, C.; Bucksbaum, P.; Coslovich, G. et al Probing ultrafast ππ*/nπ* internal conversion in organic chromophores via K-edge resonant absorption. *Nature Communications* **2017,** *8* (1), 29.

TOC IMAGE

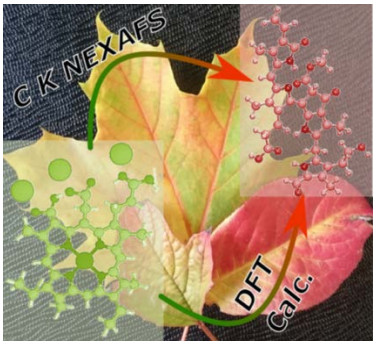

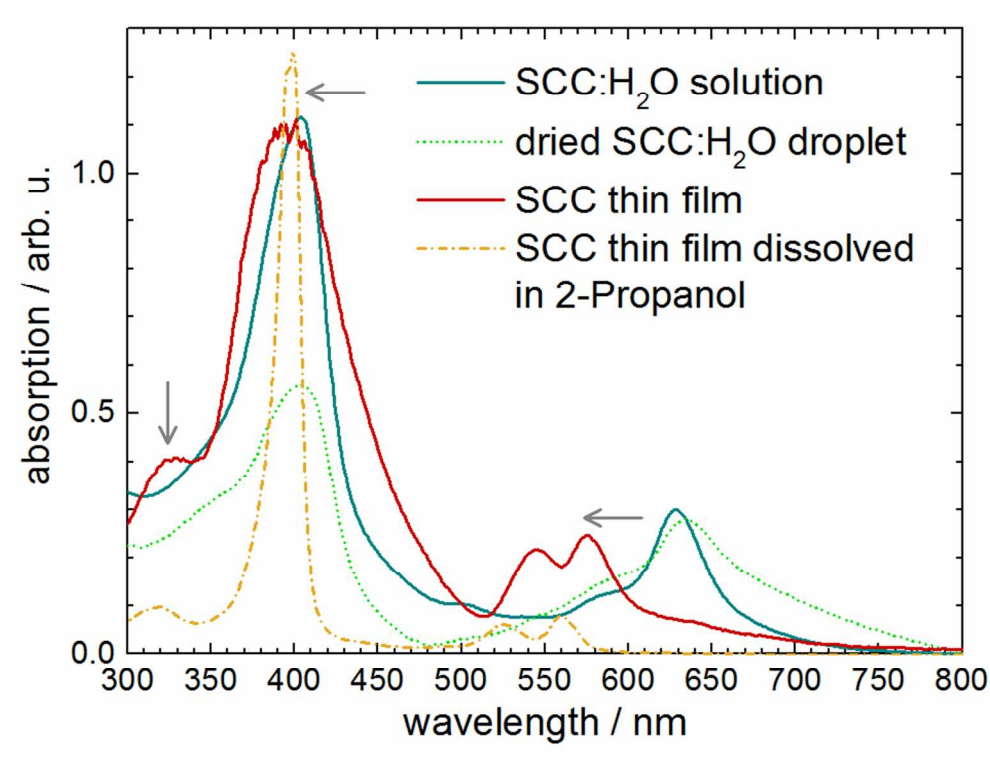

UV/VIS spectra of investigated SCC and breakdown products

82x63mm (300 x 300 DPI)

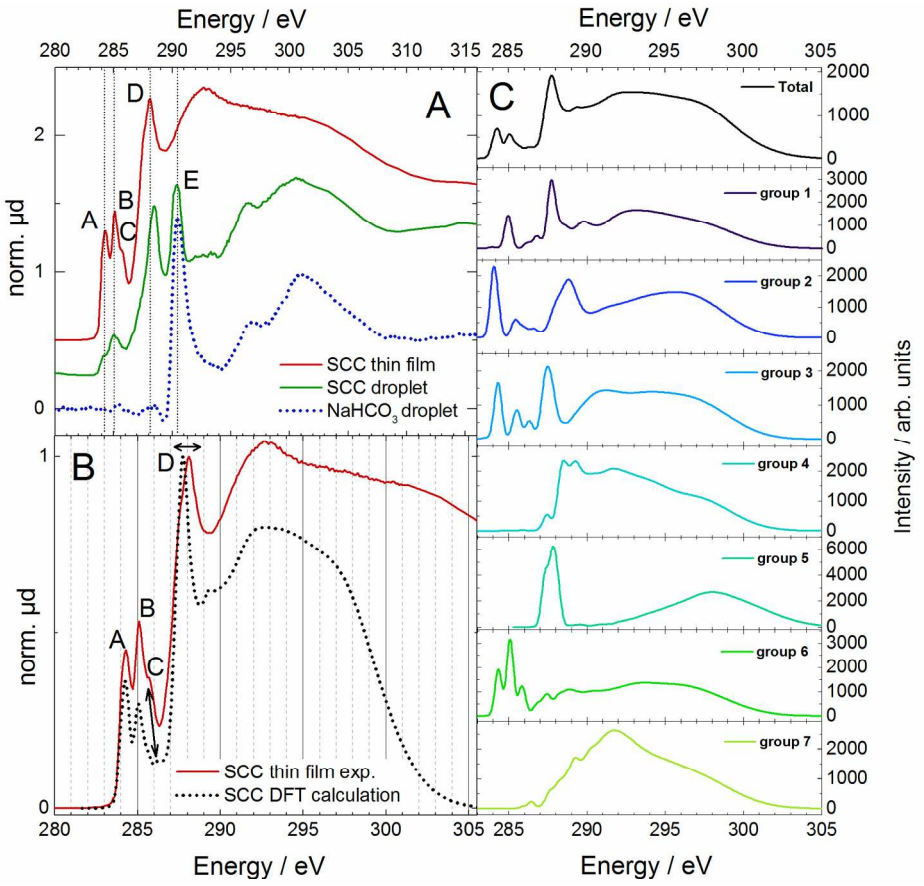

D

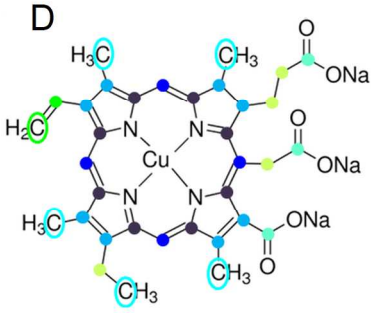

	chemical binding	peak contribution
group 1	C-N, C=N	B, C, D
group 2	-CH-, bound to two C`s within the porphyrin ring	A, B, C
group 3	C, bound to three C`s within the pyrrole ring	A, B, C, D
group 4	$-CH_3$	D
group 5	C-O, C=O	D
group 6	C=C, side chain	A, B, C
group 7	$-CH_{2^-}$, side chains	> 290 eV

NEXAFS spectra of SCC, breakdown products and reference samples compared to denstiy functional theory calculations and the resulting assigment of NEXAFS features to bonds of the SCC molecule.

177x230mm (300 x 300 DPI)

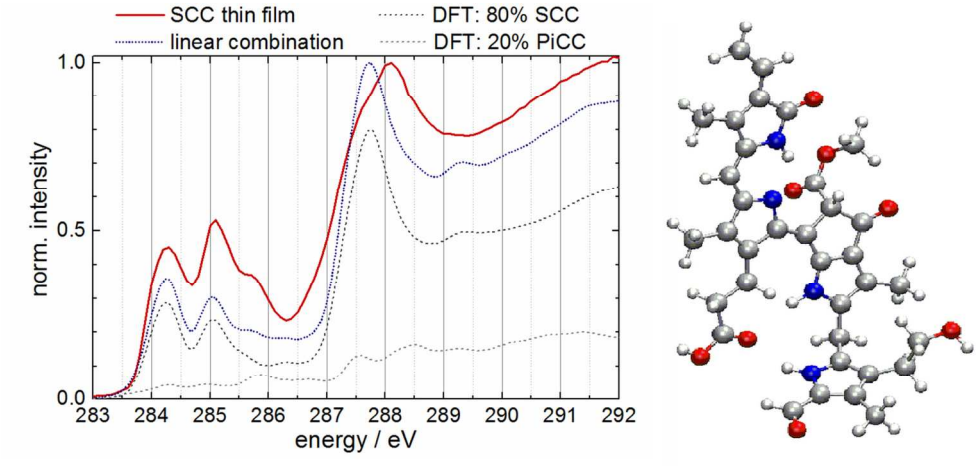

Comparison between SCC thin film NEXAFS spectrum and a linear combination of DFT calcualtions of SCC and the breakdown product PiCC.

177x82mm (300 x 300 DPI)

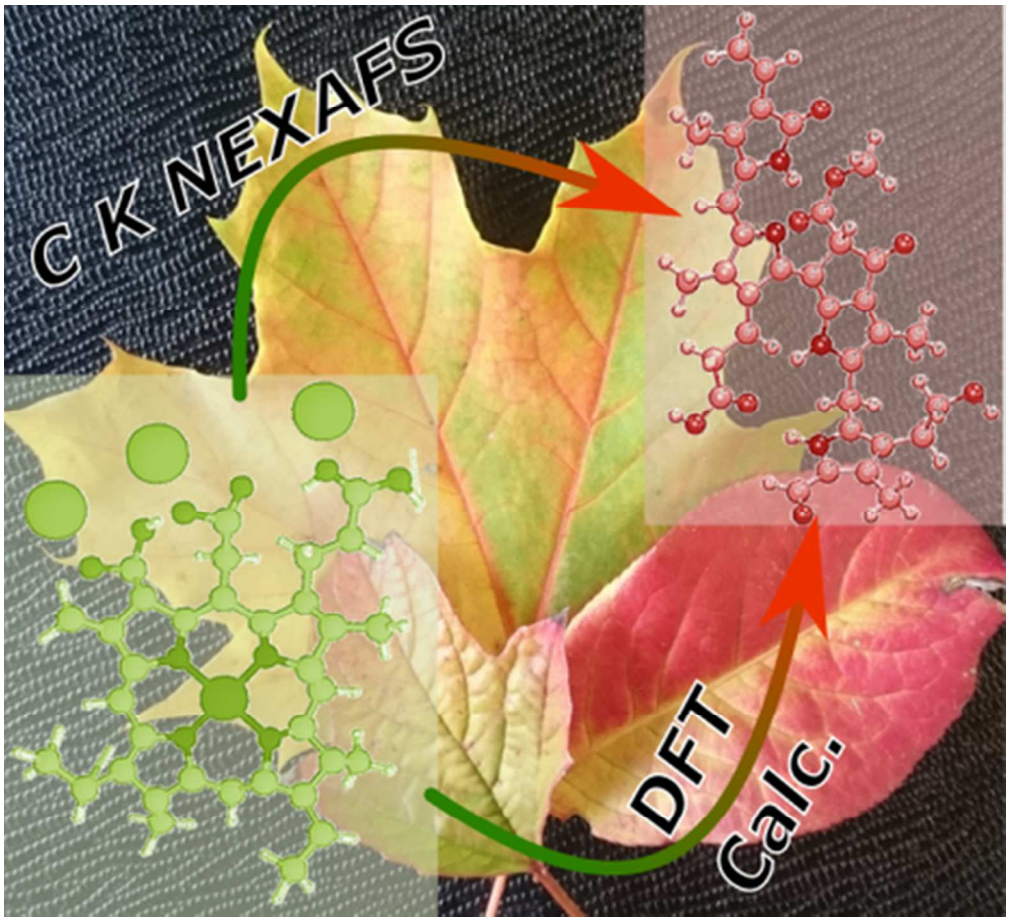

TOC graphic

50x45mm (300 x 300 DPI)